Nature of the Spin Liquid State of the Hubbard Model on a Honeycomb Lattice

B. K. Clark,[1,2] D. A. Abanin,[1,2] and S. L. Sondhi[2]

[1]*Princeton Center for Theoretical Science, Princeton University, Princeton, New Jersey 08544, USA*
[2]*Department of Physics, Joseph Henry Laboratories, Princeton University, Princeton, New Jersey 08544, USA*

(Received 21 October 2010; revised manuscript received 23 June 2011; published 17 August 2011)

Recent numerical work [Z. Y. Meng *et al.*, Nature (London) **464**, 847 (2010)] indicates the existence of a spin liquid (SL) phase that intervenes between the antiferromagnetic and semimetallic phases of the half filled Hubbard model on a honeycomb lattice. To better understand the nature of this exotic phase, we study the quantum $J_1 - J_2$ spin model on the honeycomb lattice, which provides an effective description of the Mott insulating region of the Hubbard model. Employing the variational Monte Carlo approach, we analyze the phase diagram of the model. We find three phases—antiferromagnetic, an unusual Z_2 SL state, and a dimerized state with spontaneously broken rotational symmetry. We identify the Z_2 SL state as the likely candidate for the SL phase of the Hubbard model.

DOI: 10.1103/PhysRevLett.107.087204 PACS numbers: 75.10.Kt

Introduction.—The Hubbard model describes electrons hopping on a lattice and interacting via on-site Coulomb interactions,

$$H = -t\sum_{\langle ij\rangle,s} a_{is}^{\dagger}a_{js} + U\sum_{i} n_{i\uparrow}n_{i\downarrow}, \tag{1}$$

where $s = \uparrow, \downarrow$ denotes spin and $n_{is} = a_{is}^{\dagger}a_{is}$. Despite its conceptual simplicity, the Hubbard model exhibits a rich phase diagram and is believed to capture the physics of the high-temperature cuprate superconductors [1] (for a review, see Ref. [2]). At half-filling and strong repulsion, $U \gg t$, the Hubbard model is in a Mott insulator phase, in which electrons are localized by strong Coulomb repulsion. The Mott insulator is characterized by a charge gap of the order U, and, in the limit $t \ll U$ the low-energy dynamics of this phase is associated with the spin degree of freedom. The effective spin-spin interactions, which originate from virtual hopping processes and intertwine spins of neighboring electrons, become increasingly frustrated as the ratio U/t is lowered and the Mott transition is approached. In the vicinity of the Mott transition, the frustration enhances quantum fluctuations, which can prevent ordering of spins down to zero temperature, giving rise to spin liquid (SL) ground states. The interest in SLs stems from the fact that some of them exhibit new types of topological order [3], and the fact that their properties may be linked with the physics of the doped Hubbard model [2].

Recently, the Hubbard model on the honeycomb lattice at half-filling was studied using the determinantal quantum Monte Carlo (DQMC) method [4]. This model has a crucial advantage of being free of the sign problem, and therefore the DQMC method gives essentially exact results for correlators of the system. It was found that in the vicinity of the Mott transition, the system exhibits a disordered spin phase. This phase intervenes between the antiferromagnetic Néel state realized at higher $U/t \approx 4.3$, and the semimetallic phase at $U/t < 3.5$. The authors of Ref. [4] found that the disordered phase shows a small but finite spin gap, and preserves translational symmetry and time-reversal symmetry. This suggests that the disordered state on the honeycomb lattice is a nonchiral SL.

In this Letter, we attempt to elucidate the nature of the SL state on the honeycomb lattice. We study the effective $J_1 - J_2$ spin model of the large-U Hubbard model. Using the variational Monte Carlo (VMC) method, we find a phase diagram (Fig. 1), which leads us to identify the exotic phase seen in the Hubbard model as the sublattice pairing state (SPS), a small-gap Z_2 SL, first considered in Refs. [5–7]. Our results should be contrasted with the mean-field analysis of Ref. [5] which favors a gapless SL, rather than a SPS, in the relevant parameter range. We attribute the difference to the fact that the mean-field approach [5] neglects essential gauge fluctuations, which are accounted for by VMC.

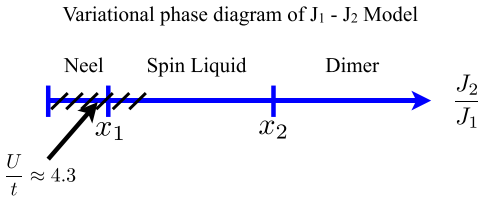

FIG. 1 (color online). Phase diagram of the quantum $J_1 - J_2$ model, obtained using the variational Monte Carlo method. As J_2/J_1 increases, the system undergoes a phase transition between an AFM state, and a gapped SL. We estimate the critical value of $J_2/J_1 = x_1 \approx 0.08$. The arrow indicates the location for this transition in the Hubbard model [4]. The SL state is best described variationally by SPS. At higher $J_2/J_1 = x_2$ the SL gives way to a dimerized phase. Our variational study gives an estimate $x_2 \approx 0.3$. The hashed area indicates values of J_2/J_1 that correspond to values of U/t in the Hubbard model that are in the Néel or SL state [4].

Spin Hamiltonian.—We start from an effective spin Hamiltonian, the $J_1 - J_2$ spin model,

$$H = J_1 \sum_{\langle ij \rangle} \mathbf{S}_i \cdot \mathbf{S}_j + J_2 \sum_{\langle\langle ij \rangle\rangle} \mathbf{S}_i \cdot \mathbf{S}_j, \tag{2}$$

where $\langle ij \rangle, \langle\langle ij \rangle\rangle$ denote nearest-neighbor and next-nearest-neighbor sites. To establish the connection with the Hubbard model, we calculate the parameters of the spin model from the perturbation theory in $(t/U)^2$ [8], finding, to second order in $(t/U)^2$, $J_1 = 4\frac{t^2}{U} - 16\frac{t^4}{U^3}$, $J_2 = 4\frac{t^4}{U^3}$. The SL phase in the Hubbard model then ranges from $J_2/J_1 \approx 0.07$ at the antiferromagnetic (AFM) transition to $J_2/J_1 \approx 0.12$ at the semimetal transition. Note that taking into account higher-order terms in the perturbation theory in $(t/U)^2$ somewhat alters the values J_2/J_1 which correspond to the SL in the Hubbard model [9]. Both exchange couplings are antiferromagnetic; thus, the effective spin model is frustrated. In this study we ignore higher-order terms in $(t/U)^2$ as well as third nearest-neighbor and ring exchange terms [10]. At the relevant $U/t \approx 4.3$ higher-order terms are likely too small to affect the results and third nearest-neighbor terms are nonfrustrating and will primarily renormalize the effective J_1.

Quantum fluctuations are particularly important in this model as they are enhanced by the low coordination number of the honeycomb lattice and competition between the J_1 and J_2 exchange interactions. We contrast the phase diagram of the quantum model (Fig. 1) with that of the classical $J_1 - J_2$ model. The latter model exhibits just two phases: AFM, with opposite spin polarization on the two sublattices of the honeycomb lattice, and (an incommensurate) spiral ordering [11,12], with a phase transition occurring at $J_2/J_1 = 1/6$. We find that the quantum fluctuations drastically alter this phase diagram. The spiral phase is destroyed at intermediate J_2/J_1, giving way to a SL phase at $J_2/J_1 < 0.3$, and a dimerized phase at $J_2/J_1 \gtrsim 0.3$. The Néel state survives at small $J_2/J_1 \lesssim 0.08$, albeit with reduced magnetization. The transition point between AFM and SL may be underestimated in our variational study; exact diagonalization studies on small clusters [13,14] suggest that the transition happens at slightly higher value of J_2/J_1.

Ansätze.—The main goal of this work is to understand the nature of the SL phase. Toward that end we focus on two primary types of wave functions: (generalized) Huse-Elser [15–18] states and resonating valence bond (RVB) states [19,20]. The former of these is chosen as a good ansatz for the AFM state. In the Huse-Elser wave function, the phase of the wave function is fixed by the Marshall sign rule and for the real part we optimize a separate variational two-body parameter $C(\mathbf{r})$ for each unique vector $\mathbf{r}$.

The RVB state is represented as

$$|\psi_{\mathrm{RVB}}\rangle = \sum_{\{\mathcal{D}\}} \mathcal{A}_{\mathcal{D}} \prod_{i,j} |\uparrow_i\downarrow_j - \downarrow_i\uparrow_j\rangle \tag{3}$$

where $\{\mathcal{D}\}$ is a (generically non-nearest neighbor) dimer covering of the lattice. Different choices for $\mathcal{A}_{\mathcal{D}}$ correspond to qualitatively different types of wave functions. RVB states are good ansätze for (gapped and gapless) spin-liquid states as well as dimer states.

One approach for selecting these amplitudes is to write down a large (but not complete) set of parameters specifying the RVB amplitudes and then optimize over them. We parameterize $\mathcal{A}_{\mathcal{D}}$ so as to be able to represent all BCS Gutzwiller-projected states [19]. We call these generic RVB states. Optimization for these (and the Huse-Elser) states is done via stochastic optimization [21]. Because optimization of a large set of parameters runs the risk of being stuck in local minima, we are not guaranteed to find the best state. Therefore, we also generate RVB amplitudes in a more physically motivated way allowing for fewer parameters.

This alternative approach uses the Schwinger fermion representation of the spin model combined with Gutzwiller projection [19]. In this approach, the spin operator on the ith site is related to fermionic creation-annihilation operators f, $f^\dagger$ as follows, $S_i^\alpha = \sum_{s,s'} f_{is}^\dagger \sigma_{ss'}^\alpha f_{is'}$, and a constraint of one fermion per site is imposed, $\sum_s f_{is}^\dagger f_{is} = 1$. Wave functions of the spin model are obtained by Gutzwiller projection of the fermionic many-body wave functions, which projects out sites with double or no occupancies.

The fermionic wave functions are then generated as ground states of a quadratic Hamiltonian on the honeycomb lattice

$$H_F = -t \sum_{\langle ij \rangle, s} f_{is}^\dagger f_{js} + \sum_{ij} \Delta_{ij} (f_{i\uparrow}^\dagger f_{j\downarrow}^\dagger - f_{i\downarrow}^\dagger f_{j\uparrow}^\dagger) + \mathrm{H.c.} \tag{4}$$

which includes nearest-neighbor hopping, and superconducting pairing. The parameters $\{\Delta\}$ are chosen in such a way that the ground state energy of the projected wave function is minimized.

An important advantage of the Schwinger fermion representation is that there exist simple choices of $\{\Delta\}$, with hopping matrix elements between nearby neighbors which describe different types of candidate SL states. Lee and Lee [22], and later Hermele [23] conjectured the existence of an algebraic spin liquid (ASL) on the honeycomb lattice, which is characterized by gapless spin excitations with a Dirac-like spectrum, similar to that in graphene. This corresponds to the nearest-neighbor tight-binding model, with $\Delta_{ij} = 0$ for all i, j. Very recently, Lu and Ran [5] analyzed possible SLs in the SU(2) PSG framework [24]. Here we will consider their candidate for a fully gapped SL—the sublattice pairing state (SPS) [25] as well as the s-wave SL (sSL) although the latter is believed to exhibit valence bond order beyond mean field. sSL is obtained by considering real Δ_{ij}'s, which are rotationally and translationally invariant, for sites i, j which are nth nearest neighbors or closer. SPS is characterized by complex pairing amplitudes, with opposite phases on the two sublattices

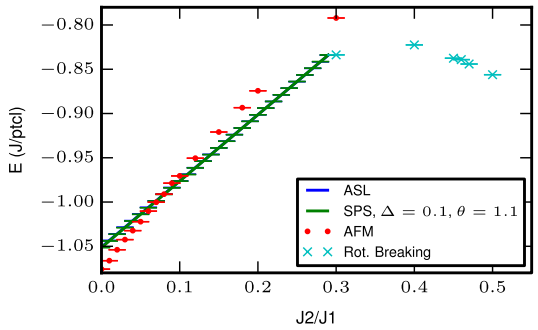

FIG. 2 (color online). Energies of AFM, ASL, SPS, and dimerized phases compared for a 10×10 system. The AFM state is favorable at $J_2/J_1 \lesssim 0.08$; ASL and SPS states have energies lower than the AFM state at $J_2/J_1 \gtrsim 0.08$, but their energies are very close. Spontaneous breaking of the rotational symmetry occurs at $J_2/J_1 \approx 0.3$, giving rise to the dimerized state.

[5], $\Delta_{ij} = \Delta e^{i\theta}$, $i, j \in A$, $\Delta_{ij} = \Delta e^{-i\theta}$, $i, j \in B$ where i, j are next-nearest neighbors. In all the SL ansätze, the symmetries (translational, time-reversal, rotational symmetry) of the honeycomb lattice are respected.

Results.—Using the VMC approach, we have mapped out the energies of various phases, illustrated in Fig. 2. We find a phase transition between AFM and SL at $J_2/J_1 \approx 0.08$. Both phases are also found in the Hubbard model [4], and the transition point is remarkably close to that in the Hubbard model. At higher frustration parameters ($J_2/J_1 > 0.3$), we find the rotational symmetry of the RVB states is broken giving a dimerized state a lower energy then that of the SL phase. This is seen by optimizing RVB amplitudes up to third nearest neighbors (with the other amplitudes fixed as in the ASL state) and is consistent with findings from exact diagonalization and spin-wave studies ([12–14]) where dimerized states have been suggested. Having identified the location of the SL phase, we turn to identifying its nature.

In establishing the form of SL state, we focus on the ASL and the SPS state, which is variationally the lowest gapped state we find. We do not consider sSL as our optimization over generic RVB states (which includes sSL) does not find a lower state then SPS. We notice that the energy difference between ASL and SPS is very small, and a more careful study is needed to distinguish between them.

To establish whether SPS is more favorable than the ASL, we have optimized the SPS energy with respect to pairing amplitude and phase. We first consider $J_2/J_1 = 0.1$, and a 14×14 system. By mapping out the energy as a function of Δ, θ (see Fig. 3), we have established the optimal values $\Delta/t \approx 0.1$, $\theta \approx 1.1$.

The energy of the SPS state with those parameters is lower than that of ASL, suggesting that ASL is unstable with respect to pairing that opens a gap. However, the energy gain due to the gap opening is so small that one may doubt whether it survives in the thermodynamic limit. To answer this question, we studied scaling of the energy

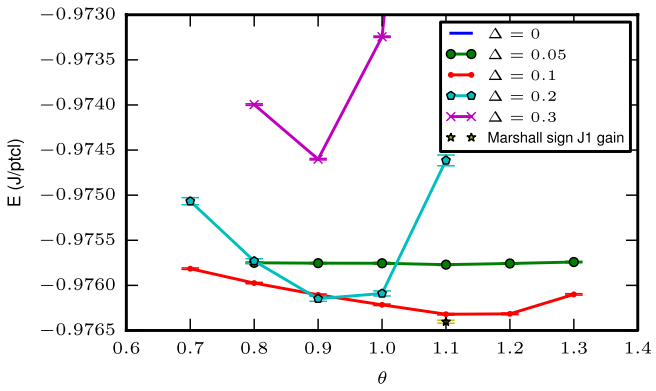

FIG. 3 (color online). Energies of the SPS state for different values of pairing amplitude Δ as a function of pairing phase θ compared to the ASL energy (for system size 14×14). The SPS state is favored, and its energy is minimized for $\Delta \approx 0.1$, $\theta \approx 1.1$. * denotes energy gain in J_1 if SPS exactly obeyed the Marshall sign.

difference $E_{\mathrm{SPS}} - E_{\mathrm{ASL}}$ at the parameter values $\Delta/t = 0.1$, $\theta = 1.1$ as a function of system size L. The result, illustrated in Fig. 4, clearly shows that the energy difference extrapolates to a nonzero value in the thermodynamic limit $1/L \to 0$, indicating that SPS is the ground state.

To understand why SPS is favorable compared to other gapped spin liquids in the regime where J_1 and J_2 interactions are competing, we studied the properties of the SPS wave function. We find that, unlike a generic SL, the optimized SPS approximately satisfies the Marshall sign rule, which is a necessary property to minimize J_1 interactions. The degree to which the Marshall sign is violated can be quantified by the J_1 energy gained if, for all c, the sign (but not the amplitude) of $\Psi(c)$ is altered so as to obey the Marshall sign rule. From Fig. 3 we see this energy gain for SPS is extremely small, which implies the sign rule is nearly satisfied. Interestingly, the ASL wave function also

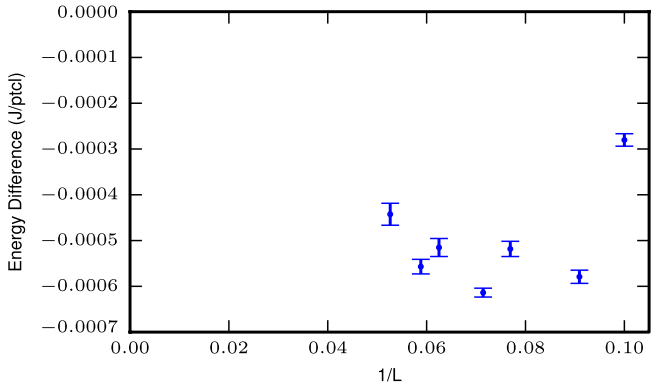

FIG. 4 (color online). Energy difference between a SPS state with optimized (for 14×14) pairing parameters ($\Delta \approx 0.1$, $\theta \approx 1.1$) and an ASL state as a function of system size. The energy difference extrapolates to a nonzero value in the thermodynamic limit $L \to \infty$. Nonmonotonicity of the points is a result of incommensurability effects with the lattice.

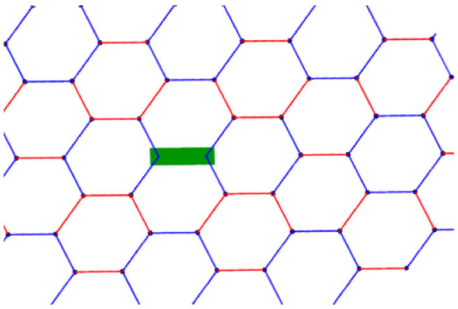

FIG. 5 (color online). Dimer-dimer correlation function, defined as in [4] for a SPS state. Green (dark gray) is the reference slice. Red (light gray) indicates a positive correlation with the reference slice and blue (medium gray) a negative correlation. The SPS has the same positive and negative correlations as the dimer-dimer correlations found in [4].

(in fact exactly) obeys the Marshall sign rule. This is a primary reason behind the ASL and SPS low energy.

We have repeated the comparison between energies for ASL and SPS in the whole range of frustration parameter $0.05 < J_2/J_1 < 0.25$, finding that SPS state is favored in the range $0.05 < J_2/J_1 < 0.2$, and at larger values of the frustration parameter the energies of the two phases are swapped. Additionally at these higher frustration parameters, we find a generic RVB state that does not break sublattice symmetry and has a lower energy then the ASL state. Because we have not studied the finite-size effects or optimized carefully the SPS parameters at these higher frustration parameters, this could either point to a series of phase transitions between the different states, or to the SPS gap becoming too small to be resolved without more careful optimization and finite size extrapolation. Further work is needed to distinguish between these different scenarios.

Having identified SPS as the variationally lowest energy state, we look at the dimer-dimer correlation function for an AFM and SL state (see Fig. 5). We find that the dimer-dimer correlations of the SL state are positively (respectively negatively) correlated on exactly the same dimers as the Hubbard model at $U/t \approx 4.0$ [4]. It should be noted that although the ASL state has a similar looking dimer pattern, due to the small gap of the SPS, the AFM state looks qualitatively different.

Discussion.—In conclusion, we have studied the $J_1 - J_2$ model on the honeycomb lattice, finding three phases—AFM, SL phase, as well as VBS phase. We have accumulated evidence that the SPS state describes the spin-liquid phase seen in the Hubbard model. Beyond having the transition happen near the correct place, we find it to be the variational lowest energy state beating out the gapless ASL state. Moreover, the dimer-dimer correlations closely match those of the Hubbard model. Finally, we should note that it is not clear whether the SPS state represents a phase of matter that is distinct from the simplest short ranged RVB phase obtained, e.g., in the quantum dimer model [26].

We thank Matthew Fisher, Duncan Haldane, David Huse, and Ronny Thomale for many invaluable discussions. D. A. A. thanks Aspen Center for Physics, where part of this work was completed, for hospitality during the program "Topological Phases." This work was partially supported by NSF Grant No. DMR-1006608 (SLS).

[1] P. W. Anderson, Science **235**, 1196 (1987).
[2] Patrick A. Lee, Naoto Nagaosa, and Xiao-Gang Wen, Rev. Mod. Phys. **78**, 17 (2006).
[3] X.-G. Wen, Phys. Rev. B **40**, 7387 (1989).
[4] Z. Y. Meng, T. C. Lang, S. Wessel, F. F. Assaad, and A. Muramatsu, Nature (London) **464**, 847 (2010).
[5] Yuan-Ming Lu and Ying Ran, arXiv:1005.4229.
[6] Fa Wang, Phys. Rev. B **82**, 024419 (2010).
[7] Y. M. Lu and Y. Ran, arXiv:1007.3266.
[8] A. H. MacDonald, S. M. Girvin, and D. Yoshioka, Phys. Rev. B **41**, 2565 (1990).
[9] H-Y. Yang and K. P. Schmidt, Europhys. Lett. **94**, 17004 (2011).
[10] Because the smallest ring exchange term involves six sites, we suspect that large energy differences are almost certainly robust against it. Small energy differences (as we find between different spin liquids) may be sensitive to its presence.
[11] S. Katsura, T. Ide, and Y. Morita, J. Stat. Phys. **42**, 381 (1986).
[12] A. Mulder, R. Ganesh, L. Capriotti, and A. Paramekanti, Phys. Rev. B **81**, 214419 (2010).
[13] J. B. Fouet, P. Sindzingre, and C. Lhuillier, Eur. Phys. J. B **20**, 241 (2001).
[14] H. Mosadeq, F. Shabhazi, and S. A. Jafari, Phil. Trans. R. Soc. A **368**, 5391 (2010).
[15] D. A. Huse and V. Elser, Phys. Rev. Lett. **60**, 2531 (1988).
[16] H. Changlani, J. Kinder, C. J. Umrigar, and G. K. L. Chan, Phys. Rev. B **80**, 245116 (2009).
[17] F. Mezzacapo, N. Schuch, M. Boninsegni, and J. I. Cirac, New J. Phys. **11**, 083026 (2009).
[18] L. Capriotti, A. E. Trumper, and S. Sorella, Phys. Rev. Lett. **82**, 3899 (1999).
[19] C. Gros, Ann. Phys. (N.Y.) **189**, 53 (1989).
[20] D. N. Sheng, O. I. Motrunich, and M. P. A. Fisher, Phys. Rev. B **79**, 205112 (2009).
[21] J. Lou and A. W. Sandvik, Phys. Rev. B **76**, 104432 (2007).
[22] S.-S. Lee and P. A. Lee, Phys. Rev. Lett. **95**, 036403 (2005).
[23] M. Hermele, Phys. Rev. B **76**, 035125 (2007).
[24] X.-G. Wen, Phys. Rev. B **65**, 165113 (2002).
[25] An equivalent state was found in the slave-boson approach in Ref. [6].
[26] R. Moessner and S. L. Sondhi, Phys. Rev. Lett. **86**, 1881 (2001).